A Numerical Study of Diffusive-Thermal Instability of Opposed Nonpremixed Tubular Flames

Hyun Su Bak[1] and Chun Sang Yoo[1,2,*]
[1]*Department of Mechanical Engineering, Ulsan National Institutue of Science and Technology, Ulsan 689-798, Republic of Korea*
[2]*School of Mechanical and Nuclear Engineering, Ulsan National Institutue of Science and Technology, Ulsan 689-798, Republic of Korea*

1 Introduction

The characteristics of the diffusive-thermal instability of nonpremixed tubular flame have been extensively investigated by experiments and numerical simulations with various burners [1-5]. In general, the diffusive-thermal instability of nonpremixed tubular flame occurs near the extinction limit when the Lewis number of fuel is less than unity. At the vicinity of extinction, small perturbations can induce alternating locally-weak and strong reaction regions of the tubular flame, subsequently leading to the formation of flame cells. This is primarily attributed to unbalance between the energy gain by fuel mass flux and the loss of heat from the flame's point of view. Temperature at the edge of a flame cell becomes higher than that at the middle part of it due to the strong focusing effect of fuel mass flux at the edge. Due to the same reason, the flame cells can survive beyond 1-D flame extinction limit [5]. In the present study, the instability characteristics of opposed nonpremixed tubular flames and the flame cell dynamics are investigated using 2-D high-fidelity numerical simulations together with the conventional linear stability analysis.

2 Numerical methods and initial conditions

First, 1-D non-dimensional governing equations of temperature and mass fractions of fuel and oxidizer in the radial direction are formulated with constant density assumption, which are given by:

$$u_r \frac{d}{dr}\begin{pmatrix} T \\ Y_F \\ Y_O \end{pmatrix} = \frac{1}{r}\frac{d}{dr}\left(r \frac{d}{dr}\right)\begin{pmatrix} T \\ Y_F/Le_F \\ Y_O/Le_O \end{pmatrix} + DaY_FY_Oe^{-T_a/T}\begin{pmatrix} q \\ -\alpha_F\tilde{Y}_{O,2} \\ -\alpha_O\tilde{Y}_{F,1} \end{pmatrix}, \tag{1}$$

where the boundary conditions are as follows:

$$T = T_1,\ \ Y_F = 1,\ \ Y_O = 0,\ u_r = u_{r,1},\ \ \text{at}\ \ r = r_1,$$
$$T = T_2,\ \ Y_F = 0,\ \ Y_O = 1,\ u_r = u_{r,2},\ \ \text{at}\ \ r = r_2.$$

The radial velocity u_r is given by [1]:

$$u_r(r) = \begin{cases} u_{r,1}\dfrac{r_1}{r}\sin\left(\dfrac{u_{r,2}}{u_{r,1}}\dfrac{r_2}{r_1}\sqrt{\dfrac{Q}{4}}\left(\dfrac{r}{r_2}\right)^2 + \dfrac{\pi}{2} - \dfrac{u_{r,2}}{u_{r,1}}\dfrac{r_1}{r_2}\sqrt{\dfrac{Q}{4}}\right) & : r_1 \le r < r_s \\ u_{r,2}\dfrac{r_2}{r}\sin\left(\sqrt{\dfrac{Q}{4}}\left(\dfrac{r}{r_2}\right)^2 + \dfrac{\pi}{2} - \sqrt{\dfrac{Q}{4}}\right) & : r_s \le r \le r_2 \end{cases}$$

where r_s and Q denote the location of the stagnation plane and the pressure eigenvalue, respectively, Le_F is the fuel Lewis number, Le_O is the oxidizer Lewis number, Da is the Damköhler number, q is the heat release rate, T_a is the activation energy, T_1 is the fuel stream temperature, and T_2 is the oxidizer stream temperature. The subscript 1 and 2 denote the inner fuel and outer oxidizer nozzles. To investigate the diffusive-thermal instability of the tubular flames similar to the experiments, q = 1.2,

*Correspondence to: csyoo@unist.ac.kr (Chun Sang Yoo)

T_a=8, Le_F = 0.3, Le_O = 1.0, $\alpha_F\tilde{Y}_{O,2}$ = 1.0, $\alpha_O\tilde{Y}_{F,1}$ = 0.36, r_1 = 20, r_2 = 100, and T_1=T_2 = 0.2 are specifited. The instability characteristics at different flame locations are also investigated by varyng the ratio of inner to outer velocity with the same stretch rate, $\kappa = 0.03927$. Le_F of 0.3 is also specified to induce the cellular instability of the tubular flames near the extinction limit as in experiments.

Simultaneous algebraic equations obtained by discretizing Eq. (1) with the finite difference method for a given *Da* are solved by a Newton-Raphson method and then, the solutions at different *Da* are solved with a simple continuation method. Figure 1 shows the maximum flame temperature as a function of *Da*, so-called "C-curve". The upper part of the C-curve represents the "near equilibrium regime" in Liñán's classification of diffusion flame regimes. The lower part together with the region near the extinction point can be classified as "premixed flame regime" such that the characteristics of premixed flames such as cellular instability can be observed in nonpremixed tubular flames. The 1-D extinction Damköhler number, Da_E, is found to be approximately 13950, 11977, and 10542 for $\left|u_{r,1}/u_{r,2}\right| = 1,\ 2,\ \text{and}\ 4$.

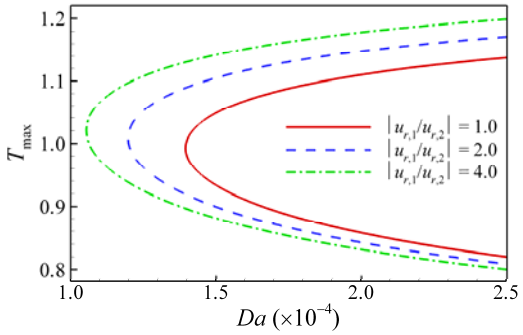

Figure 1. Maximum flame temperature as a function of Damköhler number for $\left|u_{r,1}/u_{r,2}\right| = 1,\ 2,\ \text{and}\ 4$.

To investigate the diffusive-thermal instability of 2-D opposed nonpremixed tubular flames, Eq. (1) is extended into 2-D configuration by incorporating the azimuthal direction and by assuming that there is no convective flow in the azimuthal direction:

$$\left(\frac{\partial}{\partial t}+u_r\frac{\partial}{\partial r}\right)\begin{pmatrix}T\\Y_F\\Y_O\end{pmatrix}=\left(\frac{1}{r}\frac{\partial}{\partial r}\left(r\frac{\partial}{\partial r}\right)+\frac{1}{r^2}\frac{\partial^2}{\partial\theta^2}\right)\begin{pmatrix}T\\Y_F/Le_F\\Y_O/Le_O\end{pmatrix}+DaY_FY_Oe^{-T_a/T}\begin{pmatrix}q\\-\alpha_F\tilde{Y}_{O,2}\\-\alpha_O\tilde{Y}_{F,1}\end{pmatrix} \quad (2)$$

To perform 2-D simulations, two different initial conditions (IC) are used to identify characteristics of cellular instability and dynamics with different initial states. Figure 2 shows the initial temperature fields of two different ICs: "perturbed IC" and "C-shaped IC". For the perturbed IC, 1-D solutions of *T*, Y_F, and Y_O at a given *Da* are first duplicated along the azimutal direction from 0 to 2π, and then, small pertubation of sine shape is added on top of the temperature field using Eq. (3). The perturbation amplitude constant, *A*, of 10^{-5} is adopted because the instability characteristics of tubular flames such as number of cells do not change anymore when the value of *A* becomes smaller than 10^{-5}. For the C-shpaed IC, two solutions of reacting and nonreacting flows at the same *Da* are smoothly merged using Eq. (4). This IC is used to simulate the effect of finite amplitude of perturbations on the evolution and dynamics of flame cells.

$$\mathrm{T}_{2D,\mathrm{init}}(r,\theta)=T_1+(1+A\sin\theta)\left(T_{1D}(r)-T_1\right) \quad (3)$$

$$\mathrm{x}_{2D,\mathrm{init}}(r,\theta)=\mathrm{x}_{1D,C}(r)+0.5\left[\left(\tanh(\theta-\theta_1)-\tanh(\theta-\theta_2)\right)/\sigma\right]\left(\mathrm{x}_{1D,B}(r)-\mathrm{x}_{1D,C}(r)\right) \quad (4)$$

x means solution variables where $\theta_1 = 0.5\pi$, $\theta_2 = 1.5\pi$, and $\sigma = 0.1\pi$. The subscripts B and C represent intensely-burning and cold-flow solutions.

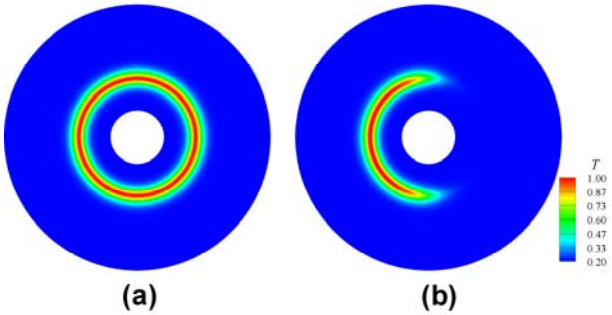

Figure 2. Two different initial temperature fields: (a) the perturbed IC and (b) the C-shaped IC.

For 2-D simulations, an 8th-order central difference scheme for spatial derivatives and a 4th-order Runge-Kutta method for time integration method are used with the massage passing interface (MPI) for parallel computing [7]. On the boundaries, Dirichlet conditions are specified in the radial direction and periodic conditions are imposed in the azimuthal direction. The grid of 400×1200 for the radial and azimuthal directions is used, and the time step is 10^{-3}.

3 Cellular instability in 2-D simulations

The 2-D opposed nonpremixed tubular flame with different initial conditions are simulated at various *Da* for $|u_{r,1}/u_{r,2}| = 1$, 2, and 4. Figure 3 shows the maximum temperature of 2-D solutions on top of 1-D "C-curve" and the number of flame cells as a function of *Da* with (a) perturbed IC and (b) C-shaped IC for $|u_{r,1}/u_{r,2}| = 1$, 2, and 4. For each cases with C-shaped IC, 2-D simulations are carried out by decreasing *Da* from 18900, 16300, and 14350 until the occurrence of total extinction. Figure 4 shows the temperature isocontours for perturbed IC cases with $|u_{r,1}/u_{r,2}| = 1$, 2, and 4 at each Da_E.

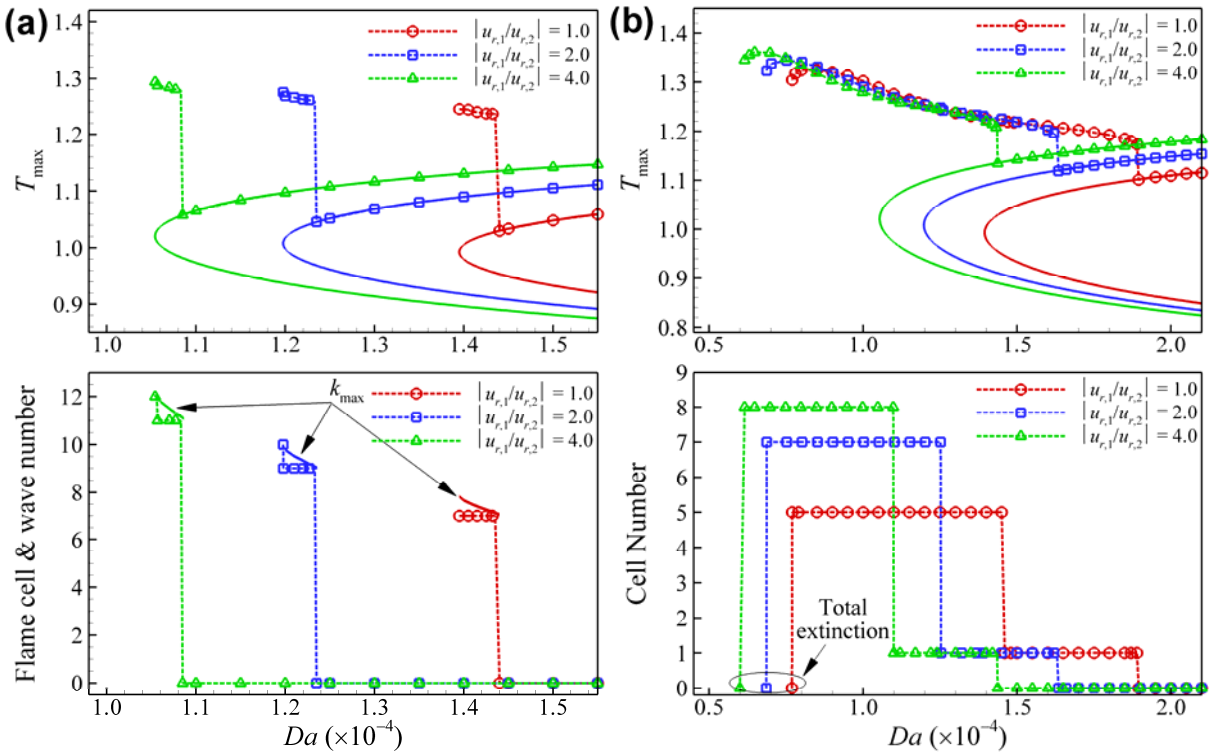

Figure 3. The maximum flame temperature and cell number as a function of *Da* for $|u_{r,1}/u_{r,2}| = 1$, 2, and 4 with (a) perturbed IC and (b) C-shaped IC.

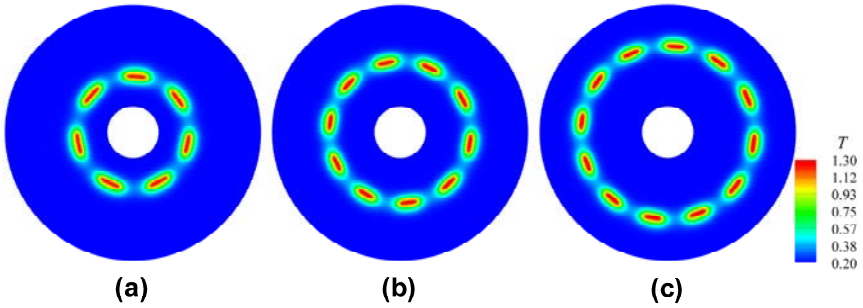

Figure 4. The temperature isocontours for cases with $|u_{r,1}/u_{r,2}| = 1$, 2, and 4 (from left to right) at each Da_E.

The occurrence of flame instability can be identified through temperature jump. For cases with perturbed IC with $|u_{r,1}/u_{r,2}| = 1$, the cellular instability occurs approximately below Da = 14412 to Da_E, and the number of cells is found to be 7 regardless of Da. For cases with $|u_{r,1}/u_{r,2}| = 2$, the onset of instability is Da = 12360, and 9 flame cells appear except nearly Da_E. For cases with $|u_{r,1}/u_{r,2}| = 4$, the cellular instability is observed from Da = 10865, and 11 flame cells are observed through the entire instability range except closely Da_E. The maximum temperatures of the flame cells are slightly increased with decreasing Da for all cases. In general, the flame cell size is reduced with decreasing Da and as such, the temperature of flame cells are increased due to more fuel focusing effect on the flame cells.

As shown in Fig. 3, for C-shaped IC cases, the cellular instability occurs approximately at Da = 18900, 16300, and 14350 for $|u_{r,1}/u_{r,2}| = 1$, 2, and 4 and just one large cell like "horseshoe-shaped", Fig. 6 (d). The detailed dynamics of this cellular flame will be discussed later in section 5. As Da is decreased, the number of flame cells is suddenly increased to 5, 7, and 8 while the maximum temperature of the cells is larger than that of 1-D case. As Da is further decreased from 18900, 16300, and 14350 for $|u_{r,1}/u_{r,2}| = 1$, 2, and 4 similar to the procedure in experiments [2, 3], it shows the same tendency with previous cases down to the extinction limit. However, 2-D extinction limit is greatly extended up to Da = 7690, 6860, and 6000, respectively. At the regime of $Da < Da_E$, the temperature of tubular flame is increased continuously with decreasing Da and the flame cell number remains the same.

4 Linear stability analysis

Linear stability of Eq. (1) is investigated by the linear stability analysis [6] to figure out the relation between the linear instability characteristics of 1-D flames and the instability of 2-D tubular flames. For linear stability analysis, the temperature and species mass fractions can be defined by a summation of the mean solution variables and perturbation in radial, azimuthal direction, and time:

$$T = \bar{T}(r) + \varepsilon T'(r) e^{ik\theta+\lambda t}, \quad Y_F = \bar{Y}_F(r) + \varepsilon Y_F'(r) e^{ik\theta+\lambda t}, \quad Y_O = \bar{Y}_O(r) + \varepsilon Y_O'(r) e^{ik\theta+\lambda t} \tag{5}$$

where the bar denotes the mean of variables, ε is a small quantity related to perturbation, λ is the amplification factor in time, and k is the wavenumber in the azimuthal direction. Substituting Eq. (5) into Eq. (2) yields the following equations:

$$\begin{aligned} &\frac{1}{r}\frac{d}{dr}\left(r\frac{d}{dr}\right)\begin{pmatrix} T' \\ Y_F'/Le_F \\ Y_O'/Le_O \end{pmatrix} - u_r\frac{d}{dr}\begin{pmatrix} T' \\ Y_F' \\ Y_O' \end{pmatrix} - \begin{pmatrix} k^2/r^2+\lambda \\ k^2/r^2Le_F+\lambda \\ k^2/r^2Le_O+\lambda \end{pmatrix}\begin{pmatrix} T' \\ Y_F' \\ Y_O' \end{pmatrix} \\ &+ Da e^{-T_a/\bar{T}}\left(\bar{Y}_O Y_F' + \bar{Y}_F Y_O' + \frac{\bar{Y}_F\bar{Y}_O}{\bar{T}^2}T_a T'\right)\begin{pmatrix} q \\ -\alpha_F\tilde{Y}_{O,2} \\ -\alpha_O\tilde{Y}_{F,1} \end{pmatrix} = 0 \end{aligned} \tag{6}$$

Equation (6) is discretized by the finite difference approximation, which leads to an eigenvalue problem of $(\mathbf{A}-\lambda\mathbf{B})\mathrm{x}'=0$, where x′ is the solution vector of T', Y_F', and Y_O'. The eigenvalue, λ, can be obtained for different wavenumber at a given Da.

Figure 5 shows the largest real eigenvalue as a function of the wavenumber for different Da with $|u_{r,1}/u_{r,2}|=1$, 2, and 4. The thin dotted segmemts represents the imaginary part of $\lambda \neq 0$. The existence of positive real eigenvalues implies that the cellular instability of tubular flame can occur because the small perturbation Eq. (5) can grow exponentially in time. From the results, the range of unstable tubular flame is approximaetly from Da = 14412, 12360, and 10865 to Da_E for $|u_{r,1}/u_{r,2}|=1$, 2, and 4, respectively. These values are almost identical to those from 2-D simulations. The maximum eigenvalues occur at the wavenumber of approximately 7.0, 9.0, and 11.0 for $|u_{r,1}/u_{r,2}|=1$, 2, and 4, respectively, which exactly coincide with the flame cell number of 2-D simulations. These results suggest that the onset of instability and the number of flame cells in 2-D tubular flames can be precisely predicted through the linear stability analysis of the corresponding 1-D flames. However, this result cannot be applicable to the charcteristics of tubular flame with C-shaped IC. This is primarily because the disturbances induced by the C-shaped IC are ~ O(1) not O(ε) and as such, the assumption of the linear stability analysis does not hold in this case. Therefore, the instability and the number of flames cells can depend highly on the shape and intensity of finite-amplitude disturbances.

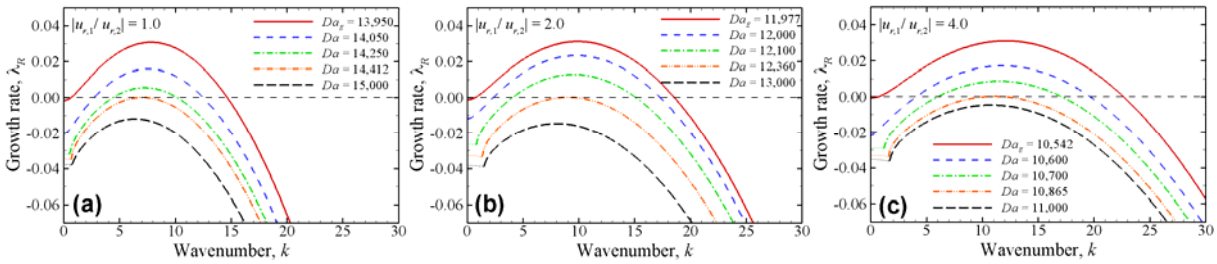

Figure 5. The largest Re(λ) as a function of wavenumber for different Da with $|u_{r,1}/u_{r,2}|$ = (a) 1 , (b) 2, and (c) 4.

5 Edge flame speed

The edge flame speed, S_d, can be defined by a sum of reaction, S_d^R, radial and azimuthal direction diffusion components, $S_{d,r}^D$and $S_{d,\theta}^D$ of a specified species [8]:

$$S_d = S_d^R + S_{d,\mathrm{r}}^D + S_{d,\theta}^D = \frac{1}{|\nabla Y_k|}\left[\dot{\omega}_F + \frac{1}{Le_k}\nabla^2 Y_k\right] \tag{7}$$

In this case, S_d is evaluated at the intersection of Y_F=0.0765 isoline and the stagnation plane. For a case using C-shaped IC at Da = 18900 with $|u_{r,1}/u_{r,2}|=1$, two edge flames developed form the initial condition propagate towards each other as shown in Fig. 6. At the steady state, however, they stand still at a short distance instead of merging to form a steady tubular flame. Figure 7 shows the temporal evolution of the displacement speed and its components. It is readily observed from the figure that after two edges are developed from the initial condition, they propagate toward each other with constant S_d. As they approach each other, S_d is decreased and finally vanishes when they stop propagation. When the two edges come to a stop, the reaction in S_d balances the diffusion as can be expected.

6 Conclusions

The characteristics of diffusive-thermal instability of opposed nonpremixed tubular flame were investigated with high-fidelity numerical simulations and linear stability analysis. 1-D steady tubular

flame solutions for $|u_{r,1}/u_{r,2}| = 1$, 2, and 4 with same stretch rate, $\kappa = 0.03927$, were first obtained by solving 1-D governing equations with the Newton-Raphson method with a simple continuation method. The 1-D solutions were then used for the initial conditions of 2-D simulations and steady-state values for the linear stability analysis. It was found from 2-D simulations that the diffusive-thermal instability occurs near the extinction points and the number of flame cells and maximum flame temperature of the cells are highly dependent on the radial location of stagnation plane and the flame cell size. It was also found that the linear stability analysis can predict precisely the number of flame cells and the *Da* at the onset of instability. From two different initial conditions, the diffusive-thermal flame instability is found to be quite sensitive to the initial conditions, especially those with finite-amplitude of disturbance. From the displacement speed analysis, the edge flame speed vanishes when the two edge flames stand still at a distance, forming a large flame cell.

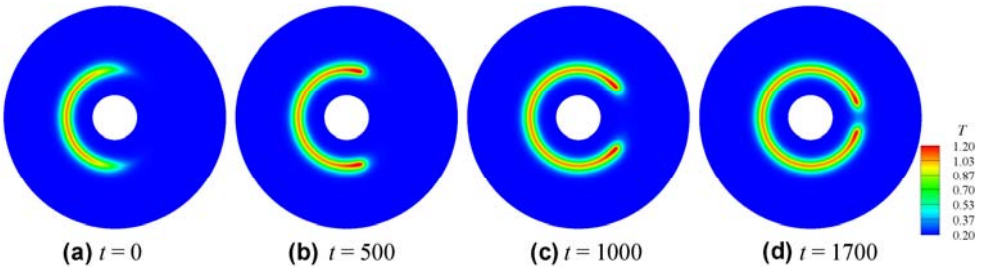

Figrue 6. The temperature isocontour variations for a case using C-shaped IC at *Da* = 18900 with $|u_{r,1}/u_{r,2}| = 1$.

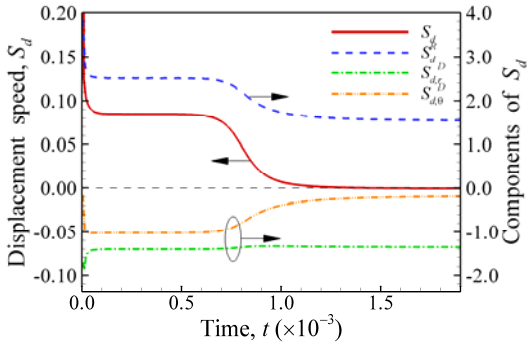

Figrue 7. The temporal evolution of the displacement speed, S_d, and its components at *Da*=18900 for $|u_{r,1}/u_{r,2}| = 1$

Acknowledgement

This work was supported by the National Research Foundation of Korea (NRF) grant funded by the Korea government (MSIP) (No. 2015R1A2A2A01007378). This research used the resources of the Supercomputing Center at Ulsan National Institute of Science and Technology (UNIST).

References

[1] P. Wang, J. A. Wehrmeyer, R. W. Pitz, Combust. Flame 145, (2006), 401-414
[2] S. Hu, P. Wang, R. W. Pitz, Proc. Combust. Inst., 31, (2007), 1093-1099.
[3] S. Hu, R. W. Pitz, Combust. Flame 156, (2009), 51-61.
[4] S. Hu, R. W. Pitz, Y. Wang, Combust. Flame 156, (2009), 90-98.
[5] S. W. Shopoff, P. Wang, R. W. Pitz, Combust. Flame 158, (2011), 876-884, 2165-2177.
[6] M. Short, J. Buckmaster, S. Kochevets, Combust. Flame 125, (2001), 893-905.
[7] C. S. Yoo, J. H. Frank, J. H. Chen, Combust. Flame 156, (2009), 140-151.
[8] H. G. Im and J. H. Chen, Combust. Flame 119, (1999), 436-454